Local and cluster critical dynamics of the 3d random-site Ising model

D. Ivaneyko [a,*], J. Ilnytskyi [b], B. Berche [c], Yu. Holovatch [b,d,a]

[a] *Ivan Franko National University of Lviv, 79005 Lviv, Ukraine*

[b] *Institute for Condensed Matter Physics, National Acad. Sci. of Ukraine, 79011 Lviv, Ukraine*

[c] *Laboratoire de Physique des Matériaux, Université Henri Poincaré, Nancy 1, 54506 Vandœuvre les Nancy Cedex, France*

[d] *Institut für Theoretische Physik, Johannes Kepler Universität Linz, 4040 Linz, Austria*

Abstract

We present the results of Monte Carlo simulations for the critical dynamics of the three-dimensional site-diluted quenched Ising model. Three different dynamics are considered, these correspond to the local update Metropolis scheme as well as to the Swendsen-Wang and Wolff cluster algorithms. The lattice sizes of $L = 10 - 96$ are analysed by a finite-size-scaling technique. The site dilution concentration $p = 0.85$ was chosen to minimize the correction-to-scaling effects. We calculate numerical values of the dynamical critical exponents for the integrated and exponential autocorrelation times for energy and magnetization. As expected, cluster algorithms are characterized by lower values of dynamical critical exponent than the local one: also in the case of dilution critical slowing down is more pronounced for the Metropolis algorithm. However, the striking feature of our estimates is that they suggest that dilution leads to decrease of the dynamical critical exponent for the cluster algorithms. This phenomenon is quite opposite to the local dynamics, where dilution enhances critical slowing down.

Key words: random Ising model, dynamical critical behaviour, critical exponents
PACS: 05.10.Ln, 64.60.Fr, 64.60.Ht 75.10.Hk

* Corresponding author.
Email addresses: ivaneiko@ktf.franko.lviv.ua (D. Ivaneyko), iln@icmp.lviv.ua (J. Ilnytskyi), berche@lpm.u-nancy.fr (B. Berche), hol@icmp.lviv.ua (Yu. Holovatch).

1 Introduction

Three-dimensional random-site Ising model (random Ising model, RIM) serves as a paradigm to describe influence of quenched dilution on systems which in a pure, undiluted, state exhibit a second order phase transition with scalar order parameter. The most prominent experimental example is given by mixed crystals $Fe_pZn_{1-p}F_2$, $Mn_pZn_{1-p}F_2$ [1] however other physical realisations of the RIM are also possible [2]. RIM offers a unique possibility to test in theory and in simulations a change of the asymptotic critical exponents caused by structural randomness. Indeed, due to the Harris criterion, the new universality class does not arise in the diluted system if the heat capacity of the corresponding pure system does not diverge (i.e. if the critical exponent $\alpha < 0$) [3]. Therefore, dilution does not change universality class of $O(m)$-symmetrical 3d systems with vector order parameter, as easy-plane or Heisenberg magnets. Such a universality test has been a challenge for numerous researchers in the on-going study since late 70-ies [1,2]. Summarized briefly, the main outcome of this research is that a new universality class has been found both in theory via renormalization group (RG) approach as well as experimentally and by Monte Carlo (MC) simulations [4].

However, the primary issue of the RIM studies performed so far concerned static critical behaviour and its numerical characteristics. Less is known about RIM critical dynamics. This paper aims to offer extensive MC simulations of the RIM dynamical critical properties. Moreover, as far as local and cluster MC algorithms correspond to different forms of dynamics, a separate task of our study is to compare numerical characteristics of Metropolis (local) and Swendsen-Wang and Wolff (cluster) dynamics for RIM. As to our knowledge the last question has never been addressed so far.

The paper is organized as follows. In the next section we give a brief summary of available theoretical and experimental data, in section 3 we introduce the model and a set of observables we are interested in. For the sake of completeness we briefly describe the MC algorithms in this section as well, simulation details are summarized in the section 4. We display and discuss the results in sections 5–7.

2 Review

In the pure (undiluted) 3d Ising model the critical slowing down, i.e. an increase of the relaxation time τ as the critical point T_c is approached, is gov-

erned by the universal dynamical critical exponent z:

$$\tau \sim |T - T_c|^{-\nu z}, \tag{1}$$

with the correlation length critical exponent ν. For isotropic systems, the dynamical exponent is related to the pair correlation function critical exponent η via $z = 2 + c\eta$ [11], where c is a (d-dependent) constant. The numerical value of the exponent η being small, the value of the dynamical exponent z for the 3d Ising model slightly differs from 2. Typical numbers are $z = 2.1(1)$ (experiment, FeF_2, [5]), $z = 2.032(4)$ (MC, [6]), $z = 2.017$ [7], $z = 2.012$ [8] (RG theories).

Below we briefly review experimental, theoretical and MC studies performed so far to analyse how the relation (1) holds for the RIM and, in particular, to answer the question how the dynamical critical exponent z is influenced by dilution. Numerical values of z that follow from our review are collected in Table 1.

Experiments. There are only three independent studies of the RIM critical dynamics we are aware of. All three concern an antiferromagnetic uniaxial crystal FeF_2 diluted by its non-magnetic isomorph ZnF_2. The resulting substance $Fe_pZn_{1-p}F_2$ was analysed by two different techniques: Mössbauer spectroscopy (studying the dynamical line broadening of the Mössbauer spectra) [9,10] and by the spin-echo neutron scattering (analyzing the time dependent spin correlation function) [5]. The earlier studies [9,5] lead to conclusion that dilution causes a decrease of z: it was found to vary from 2.1 to 1.5 when magnetic atom concentration p varied from 1 to 0.46 [9], whereas Ref. [5] reports $z = 1.7(2)$ for $Fe_{0.46}Zn_{0.54}F_2$ and explains it in the frames of conventional van Hove theory: $z = 2 - \eta$. However, a later experiment [10] brings about the value $z = 2.18(10)$ for $Fe_{0.9}Zn_{0.1}F_2$ being in a good agreement with available RG results, as we will see below.

Theory. Theoretical analysis of the RIM critical dynamics is due to the RG approach. The majority of work was devoted to analysis of the pure relaxational dynamics with non-conserved order parameter described by the Langevin equation of motion, model A dynamics in the classification of Ref. [11]. Being realized via MC simulations, it corresponds to the single spin Metropolis dynamics [12]. Change of the RIM equations of motion by coupling to the diffusive dynamics of a conserved scalar density (energy density) does not change the asymptotic critical behavior [13]: model C and model A belong to the same dynamical universality class for the RIM. However, due to crossover effects, the effective critical behaviour essentially differs for these two forms of dynamics [14].

Table 1
The dynamical critical exponent of RIM z as defined in experiments, theory and MC simulations. The methods are given in the following notations, experiments: MS, Mössbauer spectroscopy; SENS, spin-echo neutron scattering; theory: $\varepsilon^{1/2}$, first non-trivial order ε-expansion; MRG, massive RG at $d = 3$; $\overline{\rm MS}$, minimal subtraction RG at $d = 3$; Metropolis MC simulations: FSS, finite-size-scaling; DRG, dynamical RG; OE, out-of-equlibrium short-time dynamics. See the text for a whole description.

Reference	Method	Peculiarities	z
Barrett et al., 1986 [9]	MS	$Fe_pZn_{1-9}F_2$,	
		$0.46 < p < 1$	$1.5 < z < 2.1$
Belanger et al., 1988 [5]	SENS	$Fe_{0.46}Zn_{0.54}F_2$	1.7(2)
Rosov et al., 1992 [10]	MS	$Fe_{0.9}Zn_{0.1}F_2$	2.18(10)
Grinstein et al., 1977 [15]	$\varepsilon^{1/2}$		2.336
Prudnikov et al., 1992 [17]	MRG	2 loops	2.237
Janssen et al., 1995 [20]	$\overline{\rm MS}$	2-3 loops	2.18
Prudnikov et al., 1998 [18]	MRG	3 loops	2.165
Blavats'ka et al., 2005 [8]	$\overline{\rm MS}$	2 loops	2.172
Prudnikov, 1992 [32]	DRG	$L = 48$, z_M	$z(p = 0.95) = 2.19(7)$
			$z(p = 0.8) = 2.20(8)$
Heuer, 1993 [31]	FSS	$L = 60$, $z_{\lvert M\rvert,\rm int}$	2.4(1)
Parisi et al., 1999 [34]	OE	$L = 100$, z_χ	2.62(7)
Schehr et al., 2005 [26]	OE	$L = 100$, z_M	2.6(1)

The pioneering work [15] analysed by $\varepsilon = 4-d$ expansion the critical dynamics of the m-vector model with quenched random impurities and non-conserved order parameter. For the RIM case, $m = 1$, new dynamical universality class was found with the two loop value of the exponent $z = 2 + \sqrt{6\varepsilon/53}$. Being analysed at $d = 3$ naively by a simple substitution $\varepsilon = 1$ this yields $z = 2.336$ and essentially differs from z of the pure 3d Ising model quoted at the beginning of this section. However, the RG expansions are known to be asymptotic at best and resummation is needed to get reliable data on their basis [16]. Further results were obtained by the massive RG approach directly at $d = 3$ with subsequent resummation of resulting expansions: the two-loop value of the exponent reads $z = 2.237$ [17], the three-loop one is $z = 2.165$ [18]. Currently, due to essential technical difficulties, dynamical RG functions of RIM are known only within two-loop accuracy in the minimal subtraction RG scheme and within three loops in the massive RG approach at $d = 3$. In the minimal subtraction renormalization, the static RG functions were taken in three loops and combined with the two-loop expansions for the dynamic

ones. These gave the following ε-expansion for the dynamical exponent: $z = 2 + 0.336\sqrt{\varepsilon}(1 - 0.932\sqrt{\varepsilon})$ with the naive estimate $z = 2.023$ [19]. Being improved by the resummation of the static RG functions, the estimate reads $z = 2.18$ [20]. The last value is close to the other estimate, obtained from the resummation of the two-loop minimal subtraction RG functions directly at $d = 3$: $z = 2.172$ [8].

Theoretical studies mentioned above concerned dynamic criticality associated with equilibrium fluctuations. Recently, it was shown [21] that non-equilibrium relaxation at short times possess scaling features as well. In particular, if a system is suddenly quenched from high temperatures to the critical one and then released to the dynamic evolution of model A, the evolution at short times is governed by scaling laws. Both dynamical and static critical exponents can be extracted from the scaling. Short-time dynamics of the RIM at non-equilibrium critical relaxation was analysed if Refs. [25,19,26,27].

Let us mention a related problem, where an influence of quenched disorder on RIM critical dynamics was examined theoretically. These are studies of an effect of extended impurities on RIM critical dynamics [13,28,14]. As far as the presence of extended (long-range correlated) impurities changes the static universality class of RIM, the dynamical critical behaviour is found to differ from those of the RIM with point-like uncorrelated disorder.

MC simulations. Essential progress in MC simulations of static critical phenomena is due to the application of cluster algorithms [29,30]. In particular, they allowed to obtain precise values of the RIM static critical exponents [2]. It is to be emphasized here, that whereas the cluster algorithms were specially designed to lead to the same static critical behaviour as the single-spin Metropolis algorithm [12], it is not the case for dynamics. It is the Metropolis algorithm (due presumably to its locality), which leads to the same value of dynamic critical exponent as the one observed for RIM experimentally in Refs. [5,9,10] and analysed theoretically in Refs. [15,17,18,19,20,8]. In cluster algorithms, as it follows already from their name, the whole clusters of spins are flipped, which gives origin to the non-local dynamics. In its turn, the last is characterized by its own dynamical critical exponents [22,23,24]. As far as the cluster algorithms were introduced to overcome the critical slowing down, the corresponding autocorrelation times are characterized by weaker singularities as those of local dynamics: $z_{\rm cluster} < z_{\rm local}$.

Let us note, that the theoretical RG calculations assume a single dynamical critical exponent z for the relaxation times of different observables. In the MC simulations one typically finds, that the autocorrelation time of different observables is characterized by different (effective) exponents, which are expected to coincide in the asymptotics. Therefore, when we give the MC values of z in Table 1 we specify also the physical observable for which it has been mea-

sured. Already the first MC study of the RIM single-spin critical dynamics revealed dynamical scaling behaviour with a concentration-dependent critical exponent z [31]. For small dilution the following numbers were reported: $z(p = 0.95) = 2.15(1)$; $z(p = 0.9) = 2.23(1)$; $z(p = 0.8) = 2.39(1)$. The concentration dependence of z was explained by crossover. In the region of concentrations $p \simeq 0.8$ the slope of the crossover function was found to change its sign, therefore the correction-to-scaling terms were minimal. This allowed to arrive to the conclusion about an asymptotic value of the dynamic critical exponent $z = 2.4(1)$ [31]. Independently, Metropolis dynamics of the RIM was analysed in Ref. [32] by a combination of MC and dynamical RG [33] techniques. Again the concentration-dependent exponents were found with a different conclusion, however: a hypothesis of RIM step-like universality was proposed. According to the hypothesis, the asymptotic critical exponents remain unchanged only within certain concentration region. For a small dilution the values of z practically did not differ: $z(p = 0.95) = 2.19(7)$; $z(p = 0.8) = 2.20(8)$ [32] and are compatible with those obtained by a finite-size-scaling technique in Ref. [31].

Other estimates come from MC simulations of the out-of-equilibrium RIM dynamics. Here, taking into account correction-to-scaling, value $z = 2.62(7)$ was extracted from the time dependence of the out-of-equilibrium susceptibility $\chi(t)$ (with the leading dynamical correction-to-scaling exponent $\omega = 0.50(13)$) [34]. This value was further supported by the out-of-equilibrium simulations of Ref. [26], where the value $z = 2.6(1)$ was extracted from the scaling of the spin-spin autocorrelation function.

As it was noted above, the MC cluster algorithms provide different type of dynamics and therefore their scaling exponents can not be compared straightaway with those of single-spin local dynamics summarized in Table 1. Moreover, currently there is no field theory available to predict the critical exponent value for cluster dynamics even for the pure (undiluted) spin models. Study of such dynamics constitutes a separate task and certain analytical and numerical work has already been done for the pure models [22,23,24]. As to our knowledge, no results for the RIM have been obtained so far. An exception is Ref. [35], where an effective (concentration dependent) critical exponent z was obtained for the Swendsen-Wang cluster algorithm for 3d random-bond Ising model. For a small bond dilution an estimate reads: $z(p = 0.7) = 0.41$ [35].

3 Observables and MC algorithms

In our paper we consider the $3d$ Ising model with non-magnetic impurities randomly distributed over the system. The Hamiltonian of this model on the

cubic lattice has the following form

$$\mathcal{H} = -J \sum_{\langle ij \rangle} c_i c_j S_i S_j, \tag{2}$$

where $\langle ij \rangle$ denotes the summation over the nearest neighbour sites of the lattice, $c_i = 1$ if the i-th site is occupied by a spin and $c_i = 0$ otherwise, the Ising spins S_i take on the values $+1$ or -1. The spins interact via an exchange coupling J, which is positive. Occupied sites ($c_i = 1$) are considered to be uncorrelated, randomly distributed and quenched in a fixed configuration. For every observable discussed below, first the Boltzmann average with respect to the spin subsystem is performed for the fixed disorder realisation, then the averaging over different disorder realisations is performed. We will use the following notations: Boltzmann average over the spin subsystem will be denoted by angular brackets $\langle (\ldots) \rangle$ whereas the over bar $\overline{(\ldots)}$ will stand for the averaging over the disorder realisations. The number of all sites is $N = L^3$ and the number of sites carrying a spin is N_p. The concentration of spins is defined therefore as $p = N_p/N$.

3.1 The properties of interest

For a given disorder realisation, an average value of an observable $\langle \mathcal{O} \rangle$ at temperature T can be computed in the canonical ensemble from its values $\mathcal{O}$ for given spin configurations:

$$\langle \mathcal{O} \rangle = \frac{1}{\mathcal{Z}} \mathrm{Sp}\, \mathcal{O} e^{-\beta \mathcal{H}}, \tag{3}$$

where $\beta = (kT)^{-1}$, $\mathcal{Z}$ is the partition function

$$\mathcal{Z} = \mathrm{Sp}\, e^{-\beta \mathcal{H}}, \tag{4}$$

and trace in (4) is taken over the spin degrees of freedom. In the course of the MC simulation each spin configuration is generated with its proper Boltzmann weight already (more detailed description of the algorithms is given in the next section), hence the thermodynamic average is the simple average over all generated configurations. If N_{steps} is the total number of productive MC steps used for the averaging, then

$$\langle \mathcal{O} \rangle = \frac{1}{N_{\mathrm{steps}}} \sum_{\mathrm{conf}} \mathcal{O}. \tag{5}$$

Sum in (5) spans all spin configurations in which the (spin configuration dependent) observable $\mathcal{O}$ is measured.

In an ideal case of uncorrelated, statistically independent configurations, the total error in defining $\langle\mathcal{O}\rangle$ can be evaluated as

$$\langle\delta\mathcal{O}\rangle = \sqrt{\frac{\sum_{\text{conf}}(\delta\mathcal{O})^2}{N_{\text{steps}}(N_{\text{steps}}-1)}}, \tag{6}$$

where $\delta\mathcal{O} = \mathcal{O} - \langle\mathcal{O}\rangle$. In practice, however, the correlation between different spin configurations exists as the result of particular MC scheme. This correction can be characterized via the (disorder dependent) autocorrelation function [36]:

$$C_{\mathcal{O}}(\delta t) = \frac{\langle\delta\mathcal{O}(t_0+\delta t)\delta\mathcal{O}(t_0)\rangle}{\langle\delta\mathcal{O}(t_0+\delta t)\rangle\langle\delta\mathcal{O}(t_0)\rangle}, \tag{7}$$

where t_0 is some time origin.

At times large enough $C_{\mathcal{O}}(\delta t)$ decays exponentially according to the Debye law

$$C_{\mathcal{O}}(\delta t) = a\, e^{-\delta t/\tau_{\mathcal{O},\text{exp}}}, \tag{8}$$

where $\tau_{\mathcal{O},\text{exp}}$ is the exponential autocorrelation time, obtained for quantity $\mathcal{O}$ and a is a constant. Time $\tau_{\mathcal{O},\text{exp}}$ defines a time scale at which the configurations generated in a course of the MC simulation can be assumed as uncorrelated. Hence, in the simulation run of length N_{steps} MC steps, only $\frac{N_{\text{steps}}}{2\tau_{\mathcal{O},\text{exp}}}$ configurations are considered to be statistically independent.

Besides the $\tau_{\mathcal{O},\text{exp}}$, the relaxation of an observable $\mathcal{O}$ is characterized by the integrated autocorrelation time $\tau_{\mathcal{O},\text{int}}$. It is defined via

$$\tau_{\mathcal{O},\text{int}} = \frac{1}{2} + \sum_{\delta t=1}^{\infty} C_{\mathcal{O}}(\delta t)). \tag{9}$$

In practice, $\tau_{\mathcal{O},\text{int}}$ is evaluated by introducing a maximum cutoff in the sum (9) and it may be shown that both autocorrelation times coincide $\tau_{\mathcal{O},\text{int}} = \tau_{\mathcal{O},\text{exp}}$ only in the limit when this cutoff goes to $\delta t \to \infty$, otherwise $\tau_{\mathcal{O},\text{int}} < \tau_{\mathcal{O},\text{exp}}$ [38].

Let us specify now the observables we will be interested in during MC simulations. In this study we concentrate on the internal energy $\mathcal{E}$, the magnetization

$\mathcal{M}$ and absolute value of the magnetization $|\mathcal{M}|$ per site, defined as

$$\mathcal{E} = -J\frac{1}{N_p}\sum_{\langle ij\rangle} c_i c_j S_i S_j, \tag{10}$$

$$\mathcal{M} = \frac{1}{N_p}\sum_i c_i S_i, \tag{11}$$

$$|\mathcal{M}| = \frac{1}{N_p}|\sum_i c_i S_i|. \tag{12}$$

From these observables ($\mathcal{O}$) we compute the following expectation values (O):

$$E = \overline{\langle\mathcal{E}\rangle}, \qquad M = \overline{\langle\mathcal{M}\rangle}, \qquad |M| = \overline{\langle|\mathcal{M}|\rangle}. \tag{13}$$

The divergency of the autocorrelation time for any of these quantities as the T_c is approached, Eq. (1), for a finite system of size L is reflected in a power law scaling of τ with L. Taken that both exponential and integrated autocorrelation times are defined during simulation, their scaling is governed by corresponding exponents:

$$\tau_{O,\mathrm{exp}} \sim L^{z_{O,\mathrm{exp}}}, \tag{14}$$

$$\tau_{O,\mathrm{int}} \sim L^{z_{O,\mathrm{int}}}, \tag{15}$$

with O being any of the expectation values E, M, $|M|$ computed in simulations.

Note, that the theoretical RG calculations assume a unique dynamical critical exponent z for the relaxation times of all observable quantities (cf. theoretical estimates for z in Table 1). This might not hold for the scaling of the experimentally defined autocorrelation times (14), (15). For the pure system, it is believed that the scaling of autocorrelation times for the energy-like observables is described with the same dynamical critical exponent [37], the last might differ from that for the susceptibility-like observables [24].

As it was noted already above, local and cluster MC algorithms give rise to different forms of critical dynamics. Therefore, they are described by different scaling exponents (14), (15). Indeed, the large clusters of equally oriented spins are started to be formed in the vicinity of a critical point. Therefore, most of the spin update attempts made by any of local algorithms (e.g. by the Metropolis one) are wasted, and, as result, the generated configurations are highly correlated. Both the correlation time τ and the critical index z are large and system moves in a configurational space inefficiently. This poses the

severe difficulty for the calculation of the static critical exponents, but, in fact, reflects the real dynamics in the system near the critical point.

The non-local, cluster algorithms introduced by Swendsen-Wang and Wolff consider cluster pseudo-dynamics of the system by attempting to flip the whole cluster(s) at once. The primary goal is to reduce the effective autocorrelation time and, therefore, to improve the statistical sampling of generated configurations. At the same time, these algorithms bring the system into different dynamical class and an analysis of the different dynamics governed by different MC algorithms is the main goal of this study. Below, for the sake of completeness, we briefly describe main steps of the MC algorithms under consideration.

3.2 MC algorithms

The Metropolis algorithm is the simplest and historically the first MC algorithm [12]. It utilises the preferential sampling of the configurational space, where each spin configuration is generated with appropriate Boltzmann weight. The technical difficulty of generating all the new configurations independently is overcame by using instead the recipe how to produce each new configuration from the previous one. Spins are randomly selected and flipped with a probability $P = min(1, e^{-\beta\Delta H})$ where ΔH is the energy difference between the old and the new configurations. A Markovian chain of configurations is thus produced and defines the pseudodynamics of the system.

Locality of this algorithm is a serious drawback near the critical point, where large correlated clusters of spins are emerging. As the result, the vast amount of single spin flips are rejected, therefore the configurations generated are highly correlated and the system moves in a phase space inefficiently.

Cluster algorithms were designed to overcome these difficulties. They are based on the identification of clusters of sites using a bond percolation process connected to the spin configuration of the magnetic system. All spins of the clusters are then independently flipped.

In the case of the Ising model (or more generally the Potts model), the percolation process involved is obtained through the mapping onto the random graph model, first addressed by Fortuin and Kasteleyn [40]. In the Swendsen-Wang algorithm [29], a cluster update sweep consists of the following steps: depending on the nearest neighbour exchange interactions and site occupations, assign value to a bond between sites i and j with probability $P_{ij} = 1 - e^{-2\beta J c_i c_j}$, then identify clusters of spins connected by active bonds, and eventually assign a random value to all the spins in a given cluster. The spin system at criticality is mapped into a bond percolation problem at the percolation thresh-

old. It results in the producing of clusters of arbitrary large sizes, therefore the Swendsen-Wang algorithm samples the configurations in a critical region much more efficiently. This is reflected in its rather small value of the dynamical critical exponent z. Some disadvantage is an extra computer time required to split-up the system into clusters.

Wolff introduced a single cluster algorithm [30] which otherwise is much similar to the Swendsen-Wang one. A spin is randomly chosen, then the cluster connected with this spin is constructed and all the spins in the cluster are updated. Note that in this scheme, the flip of one cluster updates only the spins belonging to this cluster and therefore produces only a partial update of the system. To match the same time scale as in the Metropolis and Swendsen-Wang algorithms, the time scale of the Wolff algorithm should be corrected by a factor $c = l_{\rm cluster}/L^3$, where $l_{\rm cluster}$ is the average size of flipped clusters.

4 Simulation details

In the rest of the paper we study RIM critical dynamics governed by the three different MC algorithms described in the previous section. The MC simulations are performed for a range of system sizes up to $L = 96$ with periodic boundary conditions. The concentration of magnetic sites was fixed at $p = 0.85$. This choice is based on the previous findings that the correction-to-scaling terms are minimal at concentrations $p \sim 0.8$ [31,41]. Therefore, we do not account for these terms. The simulations are performed at the temperature that corresponds to the critical temperature of the infinite system and was taken equal to $\beta_c J = 0.2661922(83)$ according to our previous findings [42].

Table 2
CPU time (in seconds) used for performing 1000 MC steps and 10 disorder realisations.

L	10	12	16	24	32	48	64	96
Metropolis	3.33	5.81	13.77	50.17	119.26	403.69	957.72	3207.54
Sw.-Wang	3.60	6.18	14.60	55.10	130.78	442.64	1092.76	3682.48
Wolff	1.25	2.05	4.53	18.11	43.39	139.81	298.33	970.05

Typically, we averaged over $N_{\rm dis} = 10^3$ disorder realisations for each lattice size. All runs were started from a random configuration of empty and occupied spin sites. At first, we run $250\tau_{E,\rm int}$ MC sweeps for thermal equilibration and then the production run of $10^4\tau_{E,\rm int}$ MC sweeps was conducted. For all cases that was quite sufficient for the accurate description of the long-time behaviour of the autocorrelation functions.

As a basis for the random number generator we take minimal random num-

ber generator *Ran*1 of Park and Miller with Bays-Durham shuffle and added safeguards, described in Ref. [43].

We used the workstations cluster of the ICMP based on Athlon MP 2200+ processors. The typical simulation time per 1000 MC sweeps and 10 disorder realisations with data records are shown in the Table. 2.

5 Autocorrelation times

When performing the MC simulations on a system of N spins, the time unit can be related to the number of MC sweeps (MCS), where during one sweep on average N spins are updated. This convention is also used in our study. A quantitative analysis of the autocorrelation times involves an evaluation of the autocorrelation function for various properties of the system [36]. As was mentioned, in this study we concentrate on the autocorrelations of the energy $\mathcal{E}$, the magnetization $\mathcal{M}$ and the absolute value of magnetization $|\mathcal{M}|$. Defined in (7), the autocorrelation function can be rewritten as:

$$C_{\mathcal{O}}(\delta t) = \frac{\langle \delta\mathcal{O}(t_0+\delta t)\delta\mathcal{O}(t_0)\rangle}{\langle \delta\mathcal{O}(t_0+\delta t)\rangle\langle \delta\mathcal{O}(t_0)\rangle} = \\ = \frac{\langle \mathcal{O}(t_0+\delta t)\mathcal{O}(t_0)\rangle - \langle \mathcal{O}(t_0+\delta t)\rangle\langle \mathcal{O}(t_0)\rangle}{\sqrt{(\langle \mathcal{O}(t_0+\delta t)^2\rangle - \langle \mathcal{O}(t_0+\delta t)\rangle^2)(\langle \mathcal{O}(t_0)^2\rangle - \langle \mathcal{O}(t_0)\rangle^2)}}. \qquad (16)$$

In the thermodynamic limit $\langle \mathcal{O}(t_0+\delta t)\rangle$ is equal to $\langle \mathcal{O}(t_0)\rangle$, and one arrives to the more usual expression

$$C_{\mathcal{O}}(\delta t) = \frac{\langle \mathcal{O}(t_0)\mathcal{O}(t_0+\delta t)\rangle - \langle \mathcal{O}(t_0)\rangle\langle \mathcal{O}(t_0)\rangle}{\langle \mathcal{O}(t_0)\mathcal{O}(t_0)\rangle - \langle \mathcal{O}(t_0)\rangle\langle \mathcal{O}(t_0)\rangle}, \qquad (17)$$

where $\mathcal{O}(t)$ is the instant value for the property of interest at certain time t, (t_0 is some time origin, δt is the time elapsed since the time origin t_0). The averaging over a large number of time origins t_0 is needed to smoothen up the $C_{\mathcal{O}}(\delta t)$ at large δt. As an example, a typical behaviour of the energy-energy autocorrelation functions for given disorder realisations is shown in Figs. 1-3.

Table 3
The average cluster size l_{cluster} and factor c for Wolff MC algorithm

L	10	12	16	24	32	48	64	96
l_{cluster}	149	216	385	856	1526	3393	6241	15034
c	0.175	0.147	0.111	0.073	0.055	0.036	0.028	0.020

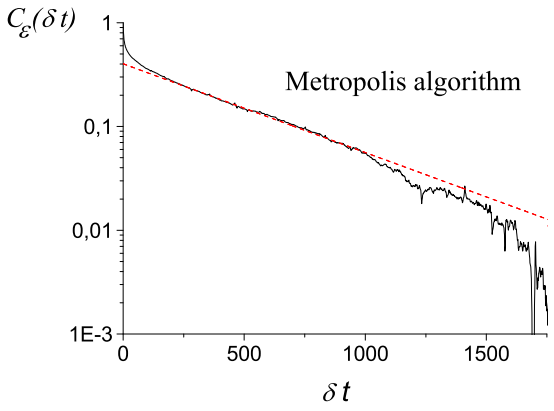

Figure 1. The log-linear plot for the energy-energy autocorrelation function $C_{\mathcal{E}}(\delta t)$, the Metropolis algorithm, $L = 64$. Bold line: measured value. Dashed line: fit to the exponential decay (8) with the autocorrelation time $\tau_{\mathcal{E},\mathrm{exp}} = 507.8$.

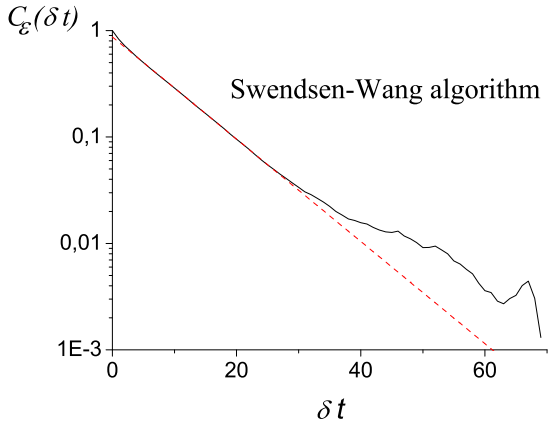

Figure 2. The log-linear plot for the energy-energy autocorrelation function $C_{\mathcal{E}}(\delta t)$, the Swendsen-Wang algorithm, $L = 64$. Bold line: measured value. Dashed line: fit to the exponential decay (8) with the autocorrelation time $\tau_{\mathcal{E},\mathrm{exp}} = 9.04$.

As was already mentioned above, the time scale of the Wolff algorithm should be accounted for the average cluster size to be compared correctly with the dynamics of other algorithms. To this end, for each lattice size and for a given disorder realisation we calculated the size of flipped cluster, skipping the first $250\tau_{E,\mathrm{int}}$ MC steps for thermal equilibration. Then we performed configurational averaging of the updated cluster size. The scaling factor c was calculated as $c = l_{\mathrm{cluster}}/N_p$, where l_{cluster} is the cluster size averaged over different disorder realisations. In Table 3, the average cluster size and the scaling factor c are presented. One could explain the behaviour of the scaling factor c by the following considerations. For the smaller system sizes, the simulation temperature (which is equal to T_c^{∞}) is much lower than the

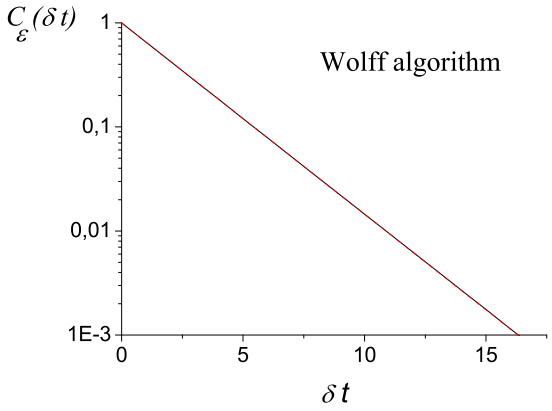

Figure 3. The log-linear plot for the the energy-energy autocorrelation function $C_{\mathcal{E}}(\delta t)$, the Wolff algorithm, $L = 64$. The measured value and the fit to the exponential decay (8) with the autocorrelation time $\tau_{\mathcal{E},\exp} = 2.63$ are indistinguishable within the scale chosen.

effective critical temperatures T_c^L, the system is at $T < T_c^L$ so that the typical cluster occupy larger part of the system. With the increase of the system size, the simulation temperature is getting closer to the T_c^L and the average clusters being flipped are decreasing in size.

To calculate the integrated autocorrelation time $\tau_{\mathcal{O},\mathrm{int}}$ the expression (9) is used. One should note that the error for the autocorrelation function is always larger at long times, where the data are averaged over less intervals. The compromised accuracy for the integrated autocorrelation time can be achieved by using certain time cutoff δt_{max}, typically of the order of $\delta t_{max} \geq 6\tau_{int}$ [38]:

$$\tau_{\mathcal{O},\mathrm{int}}(\delta t_{max}) = \frac{1}{2} + \sum_{\delta t=1}^{\delta t_{max}} C_{\mathcal{O}}(\delta t)), \tag{18}$$

The trailing part of the autocorrelation function for $\delta t > \delta t_{max}$ can be approximated by an exponential function. As the result, the final expression reads

$$\begin{aligned}\tau_{\mathcal{O},\mathrm{int}} &= \frac{1}{2} + \sum_{\delta t=1}^{\delta t_{max}} C_{\mathcal{O}}(\delta t)) + a \sum_{\delta t=\delta t_{max}+1}^{\infty} e^{-\delta t/t_{\mathcal{O},\exp}} = \\ &= \tau_{\mathcal{O},\mathrm{int}}(\delta t_{max}) + a\frac{e^{-1/\tau_{\mathcal{O},\exp}}}{1-e^{-1/\tau_{\mathcal{O},\exp}}} e^{-\delta t_{max}/\tau_{\mathcal{O},\exp}}.\end{aligned} \tag{19}$$

In this study, we employed the following scheme. For each disorder realisation the autocorrelation function $C_{\mathcal{O}}(\delta t)$ has been evaluated first. To calculate first term in (19) we use (18) with condition of the cutoff: $\delta t_{max} \geq 6\tau_{\mathcal{O},\mathrm{int}}$.

To evaluate the second term, one has to estimate $\tau_{\mathcal{O},\mathrm{exp}}$. Whereas the pure systems display asymptotic behaviour dominated by a single relaxation time, the distinct feature of the autocorrelation function of disordered systems is that there is a whole spectrum of autocorrelation times in the crossover region and it is reflected in the curvature of the autocorrelation functions in the log-log plot. This feature has been noted already in Ref. [31]. Therefore, we plot the $C_{\mathcal{O}}(\delta t)$ in log-log scale and estimated $\tau_{\mathcal{O},\mathrm{exp}}$ and a from the straight line region in a window $\tau_{\mathcal{O},\mathrm{int}}(\delta t_{max})$ to $3\tau_{\mathcal{O},\mathrm{int}}(\delta t_{max})$. The averaged over disorder realizations exponential autocorrelation time $\tau_{O,\mathrm{exp}}$ is given in Table 4 .

Table 4
Exponential autocorrelation times $\tau_{O,\mathrm{exp}}$ of RIM at the critical temperature of infinite system for different lattice sizes L measured in MC sweeps for Metropolis, Swendsen-Wang and Wolff MC algorithms.

L	Metropolis			Swendsen-Wang		Wolff	
	$\tau_{E,\mathrm{exp}}$	$\tau_{\lvert M\rvert,\mathrm{exp}}$	$\tau_{M,\mathrm{exp}}$	$\tau_{E,\mathrm{exp}}$	$\tau_{\lvert M\rvert,\mathrm{exp}}$	$\tau_{E,\mathrm{exp}}$	$\tau_{\lvert M\rvert,\mathrm{exp}}$
10	8.94(63)	9.34(88)	$6.80(1.80)\cdot 10$	3.76(19)	3.72(20)	1.53(17)	1.23(10)
12	$1.33(11)\cdot 10$	$1.40(16)\cdot 10$	$1.02(28)\cdot 10^2$	4.16(23)	4.12(21)	1.64(17)	1.30(9)
16	$2.49(24)\cdot 10$	$2.69(44)\cdot 10$	$1.98(63)\cdot 10^2$	4.82(27)	4.80(36)	1.80(21)	1.41(10)
24	$5.99(37)\cdot 10$	$6.51(95)\cdot 10$	$5.10(19)\cdot 10^2$	5.87(38)	5.92(37)	2.06(24)	1.54(10)
32	$1.12(08)\cdot 10^2$	$1.24(28)\cdot 10^2$	$1.02(57)\cdot 10^3$	6.78(52)	6.71(42)	2.20(28)	1.65(11)
48	$2.71(25)\cdot 10^2$	$2.86(40)\cdot 10^2$	$2.40(1.30)\cdot 10^3$	8.15(69)	8.02(52)	2.51(30)	1.75(10)
64	$4.65(48)\cdot 10^2$	$6.31(97)\cdot 10^2$	$4.78(2.25)\cdot 10^3$	9.19(85)	9.03(76)	2.35(21)	1.88(11)
96	$1.22(14)\cdot 10^2$	$1.44(26)\cdot 10^3$	$1.20(0.52)\cdot 10^4$	10.7(9)	10.5(9)	2.79(35)	1.99(16)

In order to calculate the error bars for the exponential and integrated relaxation times we use the blocking method. We divide all set of autocorrelation times (each corresponding to a separate replica) into n blocks so that each block contains $\frac{N_{\mathrm{dis}}}{n}$ values of the autocorrelation times. We obtain the average value and standard error due to formulas (5) and (6). Then we do simple averaging over n blocks. We do not give results for $\tau_{M,\mathrm{exp}}$ and $\tau_{M,\mathrm{int}}$ for cluster methods, because the correlation of M are absent.

6 Critical exponents

Having found autocorrelation times for different observables as functions of lattice size one can extract via Eqs. (14), (15) the values of dynamical exponents for each of the algorithms considered. Let us start with the Metropolis algorithm. Log-log plots for the integrated and exponential autocorrelation times for E, M, and $|M|$ are shown in Fig. 4. We used a linear square interpolation

Table 5
Integrated autocorrelation times $\tau_{O,\mathrm{int}}$ of RIM at the critical temperature of infinite system for different lattice sizes L measured in MC sweeps for Metropolis, Swendsen-Wang and Wolff MC algorithms.

L	Metropolis			Swendsen-Wang		Wolff	
	$\tau_{E,\mathrm{int}}$	$\tau_{\lvert M\rvert,\mathrm{int}}$	$\tau_{M,\mathrm{int}}$	$\tau_{E,\mathrm{int}}$	$\tau_{\lvert M\rvert,\mathrm{int}}$	$\tau_{E,\mathrm{int}}$	$\tau_{\lvert M\rvert,\mathrm{int}}$
10	6.14(30)	9.22(49)	6.6(1.6)·10	3.57(16)	3.22(17)	1.33(8)	0.95(4)
12	8.47(49)	1.36(8)·10	9.8(2.5)·10	3.92(18)	3.50(19)	1.42(9)	0.98(4)
16	1.44(10)·10	2.53(20)·10	1.87(53)·10^2	4.47(23)	3.95(25)	1.55(12)	1.00(4)
24	3.10(20)·10	6.13(48)·10	4.74(1.50)·10^2	5.33(31)	4.68(27)	1.75(15)	1.02(4)
32	5.51(40)·10	1.16(14)·10^2	9.05(3.41)·10^2	6.05(36)	5.14(34)	1.87(18)	1.04(4)
48	1.22(12)·10^2	2.71(28)·10^2	2.17(0.82)·10^3	7.11(47)	6.07(43)	2.08(20)	1.04(4)
64	2.15(20)·10^2	5.59(62)·10^2	3.80(1.44)·10^3	7.81(51)	6.71(50)	2.16(18)	1.07(3)
96	4.84(51)·10^2	1.24(15)·10^3	9.57(3.45)·10^3	9.21(61)	7.65(59)	2.33(25)	1.10(4)

to extrapolate the $\tau(L)$ dependencies to get the values of the exponents. To extrapolate data obtained from the Metropolis algorithm all eight data points were used, whereas for Swendsen-Wang and Wolff algorithms only five last data points (the largest system sizes) were considered.

Log-log plots for the autocorrelation time for cluster algorithms are shown in Fig. 5 (Swendsen-Wang algorithm) and Fig. 6 (Wolff algorithm). As noted above, not all autocorrelation times are well-defined for the cluster algorithms. In particular, for the Swendsen-Wang algorithm we were able to define autocorrelations for E and $|M|$ (and not for the magnetization per site M), whereas for the Wolff algorithm only $\tau_{E,\mathrm{int}}$, $\tau_{E,\mathrm{exp}}$, and $\tau_{|M|,\mathrm{exp}}$ were well-defined. However, to estimate value of the exponent $z_{E,\mathrm{exp}}$ we have to discard data for $L = 64$. As one can see from the plot in Fig. 6b an appropriate data point when included does not lead to a reasonable linear approximation.

Numerical values of the exponents are given in the first line of Table 6. With the exception of the exponent for the integrated energy autocorrelation time $\tau_{E,\mathrm{int}}$, the rest of the exponents definitely are close to the value $z \simeq 2.2$. Comparing this value with the data of Table 1 one sees, that it is in a reasonable agreement with the theoretical estimates of [15,17,18,20,8] as well as with the experimental result of [10] and data of MC simulations [31,32]. Note however, that estimates from the out-of-equilibrium MC simulations give rather different value $z \simeq 2.6$ [34,26].

A rather striking feature of the dynamical exponents of cluster algorithms is that dilution leads to decrease of the exponents, as compared to the pure 3d Ising model. Indeed, the value for the integrated dynamical critical exponent

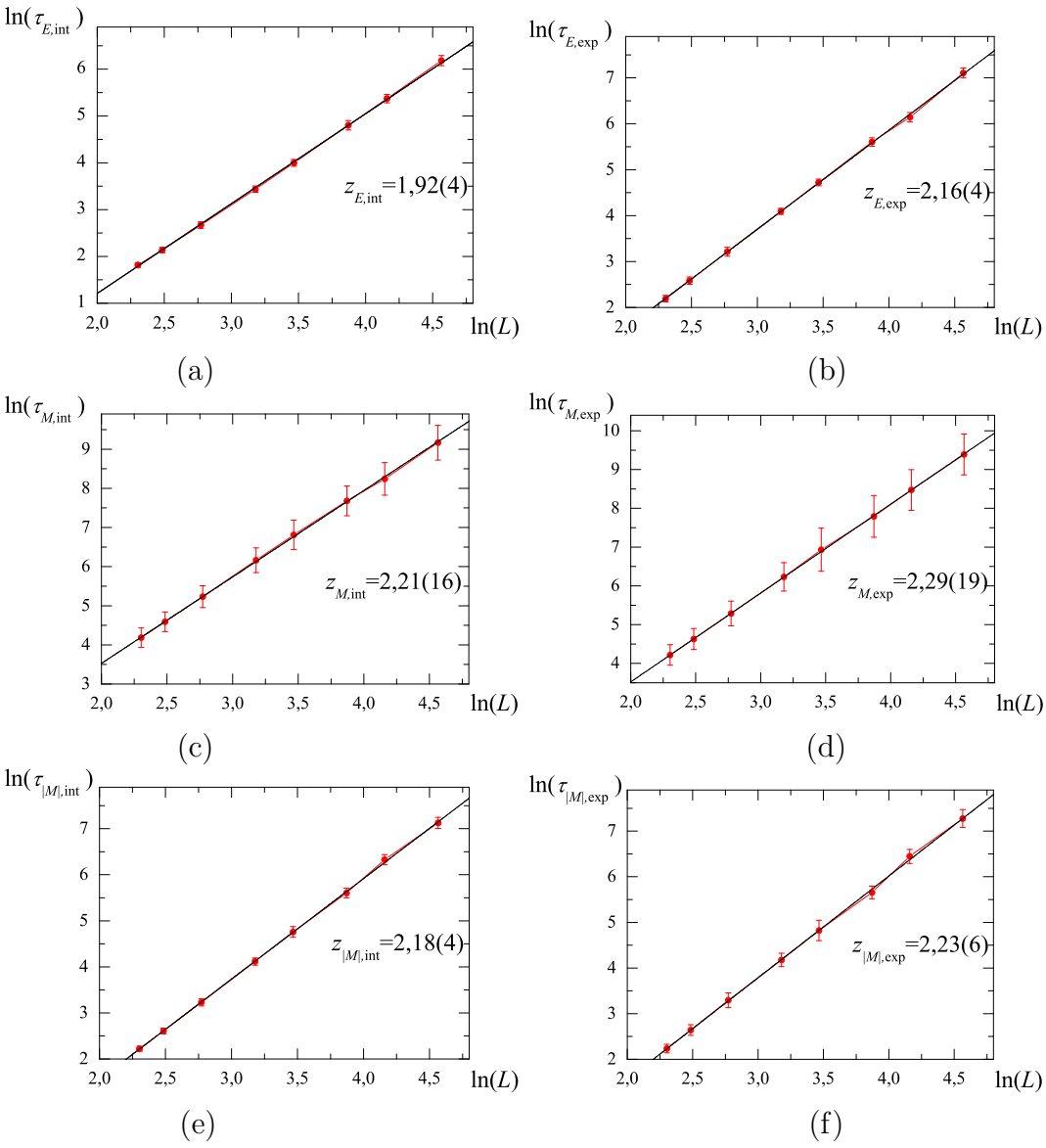

Figure 4. Integrated (left column) and exponential (right column) autocorrelation times as functions of L for the Metropolis algorithm. a,b: energy autocorrelation, $\tau_{E,\mathrm{int}}$, $\tau_{E,\mathrm{exp}}$; c,d: magnetization autocorrelation, $\tau_{M,\mathrm{int}}$, $\tau_{M,\mathrm{exp}}$; e,f: absolute value of magnetization autocorrelation, $\tau_{|M|,\mathrm{int}}$, $\tau_{|M|,\mathrm{exp}}$.

of the Swendsen-Wang algorithm for the "energy like" observables recently calculated in Ref. [24] reads: $z_{\mathcal{E},\mathrm{int}} = 0.459(30)$. In the same study, the dynamical critical exponent associated to the exponential autocorrelation time was found to be $z_{\mathrm{exp}} = 0.481$. Both values exceed those found by us for the RIM, see the second line of Table 6. Similar tendency to the dilution induced decrease of the Swendsen-Wang dynamical critical exponent was observed recently for the random-bond 3d Ising model [35]. There, the value $z = 0.41$ for the bond concentration $p = 0.7$ was found, which again is smaller than its counterpart for the pure 3d Ising model [24].

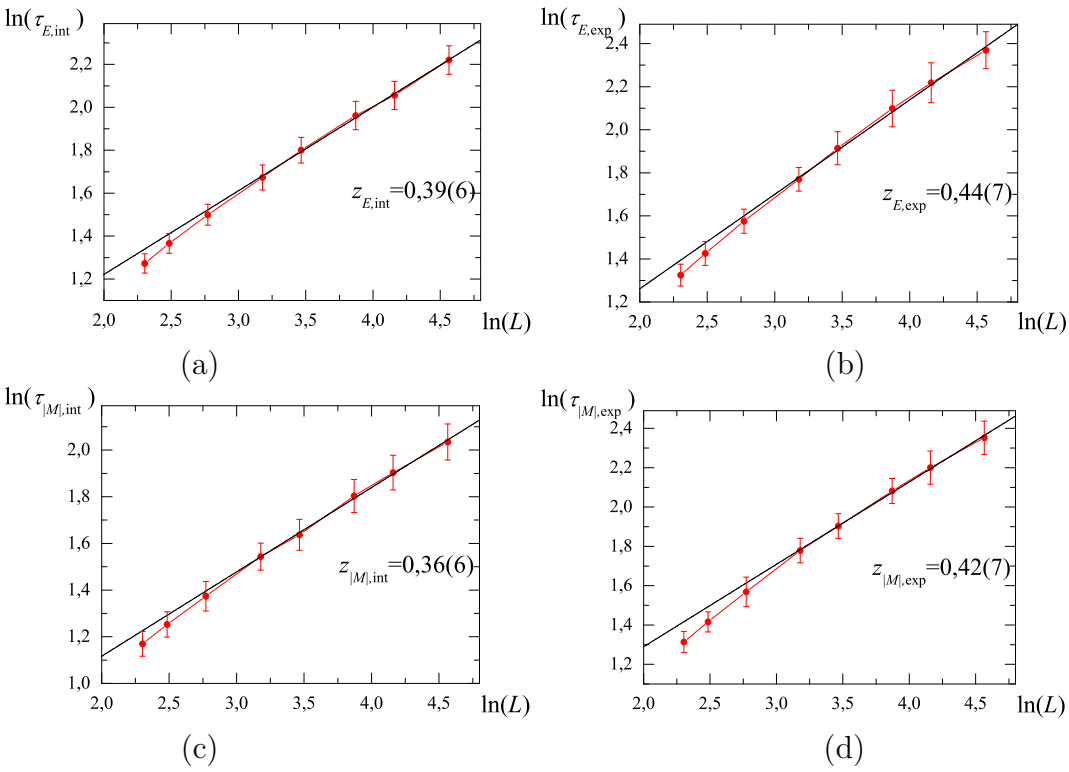

Figure 5. Integrated (left column) and exponential (right column) autocorrelation times as functions of L for the Swendsen-Wang algorithm. a,b: energy autocorrelation, $\tau_{E,\mathrm{int}}$, $\tau_{E,\mathrm{exp}}$; c,d: absolute value of magnetization autocorrelation, $\tau_{|M|,\mathrm{int}}$, $\tau_{|M|,\mathrm{exp}}$.

Table 6
RIM dynamical critical exponents for different MC algorithms, obtained from data at the critical temperature of the infinite system, Tabs. 4-5

	$z_{E,\mathrm{int}}$	$z_{E,\mathrm{exp}}$	$z_{\lvert M\rvert,\mathrm{int}}$	$z_{\lvert M\rvert,\mathrm{exp}}$	$z_{M,\mathrm{int}}$	$z_{M,\mathrm{exp}}$
Metropolis	1.92(4)	2.16(4)	2.18(4)	2.23(6)	2.21(16)	2.29(19)
Swendsen-Wang	0.39(6)	0.44(7)	0.36(6)	0.42(7)	–	–
Wolff	0.21(8)	0.22(12)	–	0.19(6)	–	–

We re-analysed simulation data, considering them at the critical temperature of a finite system of size L, $T_c(L)$. The latter may be calculated in different ways, being defined by the maximum of different observables. In Table 7, we give the values of RIM dynamical critical exponents at $T_c(L)$ obtained from the maximum of magnetic susceptibility. The critical temperature was taken from our previous study [42]. As one can see comparing Tables 6 and 7, the crossover effects do not influence data essentially.

One more question worth discussing is whether the relations between cluster algorithms dynamical exponents and the static exponents observed for the pure systems [23,22] hold for the diluted ones. Indeed, for the pure Ising model,

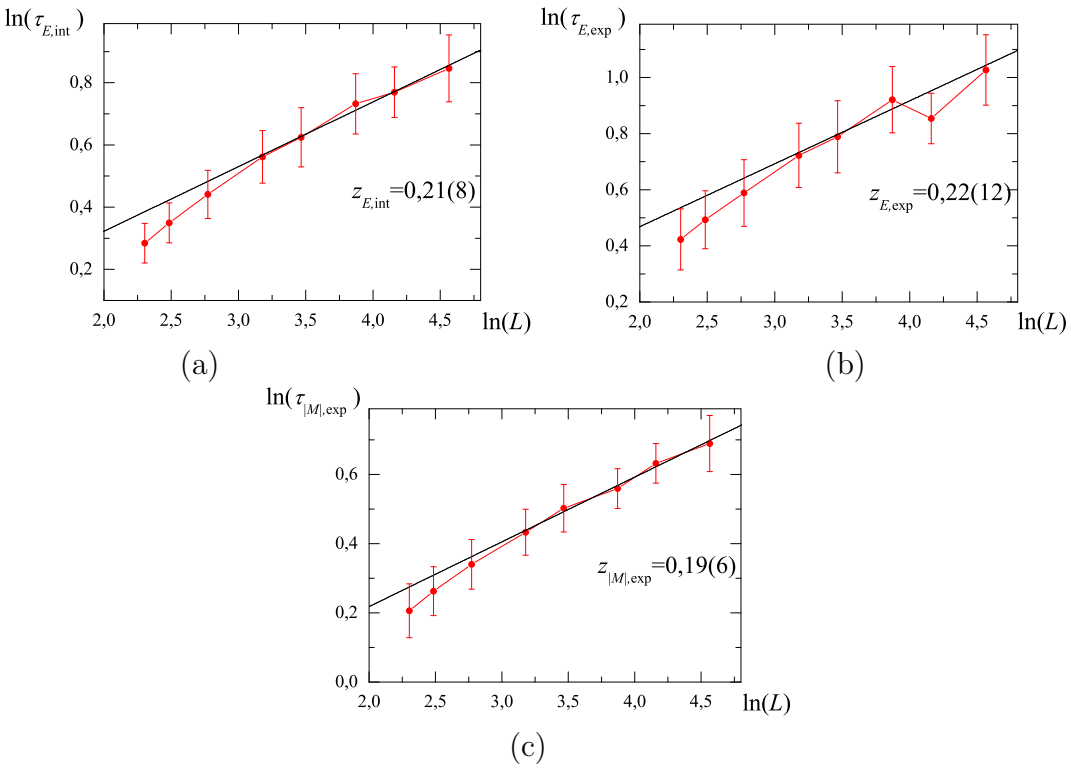

Figure 6. Autocorrelation times as functions of L for the Wolff algorithm. a,b: energy autocorrelation, $\tau_{E,\mathrm{int}}$, $\tau_{E,\mathrm{exp}}$; c: absolute value of magnetization autocorrelation, $\tau_{|M|,\mathrm{exp}}$.

Table 7
RIM dynamical critical exponents for different MC algorithms, calculated at the critical temperature of the finite size system $T_c(L)$.

	$z_{E,\mathrm{int}}$	$z_{E,\mathrm{exp}}$	$z_{\lvert M\rvert,\mathrm{int}}$	$z_{\lvert M\rvert,\mathrm{exp}}$	$z_{M,\mathrm{int}}$	$z_{M,\mathrm{exp}}$
Metropolis	1.99(3)	2.22(3)	2.19(5)	2.22(7)	2.18(12)	2.23(16)
Swendsen-Wang	0.35(5)	0.39(6)	0.32(6)	0.40(6)	–	–
Wolff	0.16(8)	0.16(9)	–	0.14(5)	–	–

the Coddington-Ballie conjecture holds [23], stating that the Swendsen-Wang dynamical critical exponent $z^{\mathrm{SW}}_{E,\mathrm{int}}$ is defined via static critical exponents for magnetization and correlation length:

$$z^{\mathrm{SW}}_{E,\mathrm{int}} = \beta/\nu. \tag{20}$$

It is worth here to note, that whereas the static critical exponents for RIM numerically differ from those of the pure 3d Ising model (cf. theoretical RG estimates $\beta = 0.349(5)$ and $\nu = 0.678(10)$ [45] for RIM with $\beta = 0.3258(14)$ and $\nu = 0.6304(13)$ [46] for pure 3d Ising model) their relation remains almost unchanged. For the numbers given above, $\beta/\nu = 0.515(15)$ for RIM and $\beta/\nu = 0.517(3)$ for the 3d Ising model. Therefore, a change in the value of the

Swendsen-Wang dynamic critical exponent upon dilution serves as an evidence that the relation (20) does not hold for RIM.

Another empirical relation found in Ref. [23] for the pure Ising model connects the dynamical critical exponent of the Wolff algorithm $z^{\rm W}_{E,{\rm int}}$ with the static ones:

$$z^{\rm W}_{E,{\rm int}} = \alpha/\nu. \tag{21}$$

As far as $\alpha < \beta$ for the 3d Ising model, comparison of Eqs. (20) and (21) leads to the inequality:

$$z^{\rm W}_{E,{\rm int}} \; < \; z^{\rm SW}_{E,{\rm int}}. \tag{22}$$

Eq. (21) does not hold for the diluted systems (where the heat capacity critical exponent is negative). However, the inequality (22) still holds, as one can see, comparing data of Table 6 for the Wolff and Swendsen-Wang algorithms. Again, the value of dynamical critical exponent for the diluted system is smaller than its counterpart for the pure one. Wolff algorithm dynamical critical exponent of the 3d Ising model found in different simulations read: $z_{E,{\rm int}} = 0.28(2)$ [47]; 0.44(10) [48]; 0.33(1) [23], all numbers exceeding those given for the Wolff case of RIM in Table 6.

7 Conclusions and outlook

In this paper, we have studied dynamical critical behaviour of the 3d random-site Ising model (RIM) originated from different MC algorithms. We considered the local single-spin Metropolis algorithms as well as Swendsen-Wang and Wolff cluster algorithms. Giving origin to an equivalent static critical behaviour, all three algorithms correspond to different forms of dynamics. A comparison of numerical characteristics of Metropolis (local) and Swendsen-Wang and Wolff (cluster) dynamics for RIM was achieved by calculation of the integrated and exponential autocorrelation times for RIM energy and magnetization.

The local update Metropolis algorithm corresponds to the pure relaxational single-spin dynamics with non-conserved order parameter and finds its theoretical description as the model A critical dynamics [11]. There exist RG analysis of critical dynamics for the RIM with such type of relaxation [15,17,18,20,19,8]. It assumes, however, a single dynamical critical exponent z for the relaxation times of different observables. Although the perturbation theory series are

divergent and only the lowest non-trivial order calculations have been performed so far, being resummed appropriately, all available theoretical data are coherent with an estimate $z \simeq 2.2(1)$ (see Table 1 of our paper). This is further supported by the latest experimental observation we are aware about, $z = 2.18(10)$ [10]. Whereas initial MC simulations gave estimates of z along with the above value [31,32], recent simulations of Refs. [34,26] favour an estimate $z \simeq 2.6(1)$. Our results for the values of RIM dynamical critical exponent for a local dynamics are summarized in the first line of Table 6. The essential features of the discussion remain unchanged, when one considers calculations at the critical temperature of the finite size system, $T_c(L)$, Table 7. Except of the exponent for the energy integrated autocorrelation time, $z_{E,\mathrm{int}}$, our data supports an estimate $z \simeq 2.2(1)$ within different error bars, corresponding to different observables measured during simulations. The discrepancy between our estimates an those of Refs. [34,26] may be caused by the fact, that the latter have defined scaling exponents for the out-of-equilibrium short-time dynamics.

The Swendsen-Wang and Wolff algorithms give rise to the dynamics of spin clusters, which differs from the local one. Even for the pure 3d Ising model there is no field theory describing such dynamics. However, there exist estimates, relating dynamical critical exponent of the cluster algorithms to the static exponents. Besides Eqs. (20), (21), the following inequality has been proven for the energy-like integrated and exponential autocorrelation time critical exponents of Swendsen-Wang algorithm [22]:

$$z^{\mathrm{SW}}_{\mathcal{E},\mathrm{int}}, z^{\mathrm{SW}}_{\mathrm{exp}} \geq \alpha/\nu. \tag{23}$$

Eqs. (20), (21), (23) hold for the pure Ising model. In particular, Eq. (23) leads to the conclusion, that systems with a positive specific heat exponent α must display critical slowing down. In absence of such inequality for the diluted system, our results for the critical dynamics of RIM for cluster algorithms prove that the critical slowing down is present in diluted systems as well. However, a striking feature of our estimates (second and third lines of table 6) is that they suggest that dilution leads to decrease of the dynamical critical exponent for the cluster algorithms. This phenomena is quite opposite to the local dynamics, where dilution enhances critical slowing down. The values of the exponents describing relaxation of different observables differ numerically, being however close to each other. Nevertheless, on this stage it is impossible to exclude that the difference is not only due to the crossover phenomena [49].

Acknowledgements

We acknowledge useful discussions with Christophe Chatelain, Maxym Dudka, Reinhard Folk, and Wolfhard Janke. Work of Yu.H. was supported in part by the Austrian Fonds zur Förderung der wissenschaftlichen Forschung, project No. 16574 PHY.

References

[1] Belanger D.P., Braz. J. Phys., 2000, **30**, 682.

[2] For a recent review of RIM critical behaviour see e.g.: Folk R., Holovatch Y., Yavors'kii T., Phys. Usp. 2003, **46**, 175. [Uspekhi Fiz. Nauk, 2003, **173**, 175].

[3] Harris A.B., J. Phys. C, 1974, **7**, 1671.

[4] About coexistence of theory, experiment and simulations for RIM see: Berche B., Berche P. E., Chatelain C., Janke W., Condens. Matter Phys., 2005, **8**, 47.

[5] Belanger D. P., Farago B., Jaccarino V., King A.R., Lartigue C., Mezei F., J. Phys. (Paris) Colloq., 1988, **49**, C8-1229.

[6] Grassberger P., Physica A, 1995, **214**, 547 (Erratum 1995, **217**, 227(E))

[7] Prudnikov V.V., Ivanov A.V., Fedorenko A.A., JETP Lett., 1997, **66**, 835. [Pis'ma Zh. Eksp. Teor. Fiz., 1997, **66**, 793].

[8] Blavats'ka V., Dudka M., Folk R., Holovatch Yu. Phys. Rev. B, 2005, **72**, 064417.

[9] Barrett P.H., Phys. Rev. B, 1986, **34**, 3513.

[10] Rosov N., Hohenemser C., Eibschütz M., Phys. Rev. B, 1992, **46**, 3452.

[11] Hohenberg P.C., Halperin B.I., Rev. Mod. Phys., 1977, **49**, 435.

[12] Metropolis N., Rosenbluth A. W., Rosenbluth M. N., Teller A. H., Teller E., J. Chem. Phys., 1953, **21**, 1087.

[13] Lawrie I.D., Prudnikov V.V., J. Phys. A, 1984, **17**, 1655.

[14] Dudka M., Folk. R., Holovatch Yu., Moser G., Phys. Rev. E, 2005, **72**, 036107; J. Phys. A (submitted).

[15] Grinstein G. Ma S.-k., Mazenko G.F., Phys. Rev. B, 1977, **15**, 5081

[16] Zinn-Justin J. Quantum Field Theory and Critical Phenomena (International Series of Monographs on Physics, 92). Oxford University Press, Oxford, 1996.

[17] Prudnikov V. V., Vakilov A. N., Sov. Phys. JETP, 1992, **74**, 990 [Zh. Eksp. Teor. Fiz., 1992, **101**, 1853].

[18] Prudnikov V. V., Belim S. V., Osintsev E. V., Fedorenko A. A., Phys. Solid State, 1998, **40**,1383 [Fiz. Tverd. Tela, 1998, **40**, 1526].

[19] Oerding K., Janssen H. K., J. Phys. A, 1995, **28**, 4271.

[20] Janssen H. K., Oerding K., Sengespeick E., J. Phys. A, 1995, **28**, 6073.

[21] Janssen H. K., Schaub B., Schmittmann B., Z. Phys. B: Condens. Matter, 1989, **73**, 539.

[22] Li X.-J., Sokal A. D. Phys. Rev. Lett., 1989, **63**, 827.

[23] Coddington P.D., Baillie C.F., Phys. Rev. Lett, 1992, **68**, 962.

[24] Ossola G., Sokal A. D., Nucl. Phys. B, 2004, **691**, 259.

[25] Kissner J. G., Phys. Rev. B, 1992, **46**, 2676.

[26] Schehr G., Paul R., Phys. Rev. E, 2005, **72**, 016105.

[27] Schehr G., Paul R., 2005, preprint cond-mat/0511571.

[28] Korutcheva E., Javier de la Rubia F., Phys. Rev. B, 1998, **58**, 5153; Fedorenko A. A., Phys. Rev. B, 2004, **69**, 134301; Chen Y., Li Z.-B., Phys. Rev. B, 2005, **71**, 174433.

[29] Swendsen R.H., Wang J.-S. Phys. Rev. Lett., 1987, **58**, 86.

[30] Wolff U., Phys. Rev. Lett., 1989, **62**, 361.

[31] Heuer H.-O., J. Phys. A, 1993, **26**, L341.

[32] Prudnikov V. V., Vakilov A. N., JETP Lett, 1992, **55**, 741 [Pis'ma Zh. Eksp. Teor. Fiz., 1992, **55**, 709].

[33] Jan N., Moseley L. L., Stauffer D., J. Stat. Phys., 1983, **33**, 1.

[34] Parisi G., Ricci-Tersenghi F., Ruiz-Lorenzo J. J., Phys. Rev. B, 1999, **60**, 5198.

[35] Berche P.E., Chatelain C., Berche B., Janke W. Eur. Phys. J. B, 2004, **38**, 463.

[36] Allen M.P., Tildesley D.J. Computer Simulation of Liquids. Clarendon Press, Oxford, 1987.

[37] Salas J., Sokal A. D., J. Stat. Phys., 1997, **87**, 1.

[38] Janke W. Statistical analysis of simulations: data correlations and error estimation. In: Quantum Simulations of Complex Many-Body Systems: From Theory to Algorithms, Lecture Notes, J.Grotendorst, D.Marx, A.Muramatsu, eds., John von Neumann Institute for Computing, Jülich, NIC Series, 2002, vol. 10, p. 423-445.

[39] Monte Carlo Methods in Statistical Physics. Edited by K. Binder (Springer-Verlag. New York, 1979; K. Kawasaki, in: Phase Transitions and Critical Phenomena. Edited by C. Domb and M. S. Green (Academik, New York, 1972) vol. 2.

[40] Kasteleyn P.W., Fortuin C. M., J. Phys. Sos. Jpn. Suppl., 1969, **26**, 11; Fortuin C. M., Kasteleyn P.W., Physica (Utrecht). 1972, **58**, 536; Fortuin C. M., Physica (Utrecht), 1972, **58**, 398: *ibid* 1972, **59**, 545.

[41] Ballesteros H.G., Fernández L.A., Martiń-Mayor V., Muñoz Sudure A., Phys. Rev. B, 1998, **58**, 2740.

[42] Ivaneyko D., Ilnytskyi J., Berche B., Holovatch Yu., Condens. Matter Phys., 2005, **8**, 149.

[43] Flannery B. P., Teukolsky S. A., Vetterling W. T.,Numerical Recipes in C : The Art of Scientific Computing, William H. Press.

[44] Ferrenberg A. M., Landau D. P., Phys.Rev. B, 1991, **44**, 5087.

[45] Pelissetto A., Vicari E., Phys. Rev. B, 2000, **62**, 6393.

[46] Guida R., Zinn-Justin J., J. Phys. A, 1998, **31**, 8103.

[47] Wolff U., Phys. Lett. B, 1989, **228**, 379.

[48] Tamayo P., Brower R. C., Klein W., J. Stat. Phys., 1990, **58**, 1083.

[49] In this context let us mention the paper Monceau P., Hsiao P.-Y., Phys. Rev. B, 2002, **66**, 104422, where an essential difference between the exponents $z_{E,\mathrm{int}}$ and $z_{M,\mathrm{int}}$ was reported for the Wolff dynamics of the Ising model on the Sierpinski fractals.